

# Raman scattering due to a one-magnon excitation process in $\text{MnV}_2\text{O}_4$

S. Miyahara,<sup>1</sup> K. Takubo,<sup>2</sup> T. Suzuki,<sup>2</sup> T. Katsufuji,<sup>2,3,4</sup> and N. Furukawa<sup>1,5</sup>

<sup>1</sup> *Multiferroics Project (MF), ERATO, Japan Science and Technology Agency (JST), Tokyo 113-8656, Japan*

<sup>2</sup> *Department of Physics, Waseda University, Tokyo 169-8555, Japan*

<sup>3</sup> *Kagami Memorial Laboratory for Material Science and Technology, Waseda University, Tokyo 169-0051, Japan*

<sup>4</sup> *PRESTO, Japan Science and Technology Agency, Saitama 332-0012, Japan*

<sup>5</sup> *Department of Physics and Mathematics, Aoyama Gakuin University, Kanagawa 229-8558, Japan*

(Dated: February 16, 2022)

Unconventional peak structure in the Raman spectra due to magnon excitation at low temperature is observed in spinel magnet  $\text{MnV}_2\text{O}_4$ , where a noncollinear spin state is realized by geometrical frustration. We propose a new mechanism to induce such a Raman scattering process due to a one-magnon excitation of the noncollinear spin state. Novel features of the scattering such as selection rules and peak position observed experimentally in  $\text{MnV}_2\text{O}_4$  can be explained quite naturally by considering the present one-magnon process. We also discuss that such one-magnon process may exist in various materials with noncollinear spin structures.

PACS numbers: 78.30.-j, 75.30.-m, 75.10.Hk, 75.25.Dk

Geometrically frustrated magnetic systems have been paid considerable attentions to because of the novel magnetic properties [1–4]. The frustration plays a role to suppress the conventional magnetic order, and stabilizes unusual ground states with unusual magnetic excitations like macroscopically degenerate ground state in classical spin systems, a spin liquid ground state and spin gap excitations in quantum spin systems. As a typical example in three dimensional case, magnetism on a pyrochlore lattice has been studied intensively more than 50 years [5], and, novel features have still been discovered both experimentally and theoretically [1, 4].

One of such frustrated system in three-dimensional system is a spinel vanadate  $\text{MnV}_2\text{O}_4$  [6–11], where a network of  $\text{V}^{3+}$  spins ( $S_B = 1$ ) makes a pyrochlore lattice. In the ground state,  $\text{Mn}^{2+}$  spins ( $S_A = 5/2$ ) and the  $\text{V}^{3+}$  spins show a noncollinear ferrimagnetic order due to the frustration. It was found that this compound reveals the phase transitions at  $T_N = 58$  K. At  $T_N$ , the magnetic moment of the Mn and V sites align to the opposite direction. At the same temperature, a structural phase transition from a cubic to a tetragonal occurs due to the orbital ordering on the V site [8, 9], where ferro-orbital ordering structure along [110] and  $[1\bar{1}0]$  V chains, and antiferro-orbital ordering along [001] directions are realized. Such an orbital structure partially relaxes the effects of the geometrical frustration for V spins. As a result, the magnetic behaviors on V spins can be described as the weakly coupled antiferromagnetic chain along [110] and  $[1\bar{1}0]$ , and induce the magnetically ordered state. [12].

In this Letter, we report Raman scattering results in  $\text{MnV}_2\text{O}_4$ . At low temperatures ( $T \ll T_N$ ), we observe a well-defined sharp peak corresponding to the magnon mode. The peak appears even in parallel light polarization, which can not induce the one-magnon scattering by conventional mechanisms [13, 14]. Alternatively, we propose a novel mechanism such that, in a noncollinear

spin structure, Raman scattering process due to single magnon excitation can also be generated for the parallel light polarization. We demonstrate that the selection rule and the peak position of the Raman scattering observed in  $\text{MnV}_2\text{O}_4$  are explained naturally by the new mechanism.

Raman scattering was measured on the cleaved (001) surface (in the cubic setting) of a  $\text{MnV}_2\text{O}_4$  single crystal, which was grown by a floating-zone technique. The 514.5 nm laser line from an Ar ion laser was used as the incident light, and the scattered light was collected into a grating spectrometer with a CCD detector. The polarization directions,  $a$  and  $b$ , are along the V-O bond, and the  $a'$  and  $b'$  are rotated by  $45^\circ$  within the plane. Since the surface is determined in the cubic setting, a light polarization in the experiment may consist of two types of polarization structures. Namely,  $(a, b)$  configuration can be  $(x, y)$  and/or  $(z, x)$ , where  $(x, y, z)$  are defined in the tetragonal setting:  $x$  and  $y$ -axes are along the longer V-O bond and  $z$  is along shorter one. Hereafter, we distinguish the representation  $(x, y, z)$  from  $(a, b, c)$  defined in the cubic structure. Symmetry argument for the observed Raman modes was performed in  $D_{4h}$  space group, since we can not distinguish  $x$  ( $y$ ) and  $z$  directions at  $T < T_N$ .

The temperature dependence of Raman shift intensities of  $\text{MnV}_2\text{O}_4$  for  $(a, b)$  light polarization is shown in Fig. 1 (a). At the lowest temperature  $T = 5$  K, a sharp peak around  $180\text{cm}^{-1}$  has been observed and the intensities of it increase by lowering the temperature below  $T_N$ . Light polarization dependence for  $(a, b)$ ,  $(a', a')$ , and  $(a', b')$  at  $T = 5$  K is shown in Fig. 1 (b). The sharp peak has been observed for both  $(a, b)$  and  $(a', a')$  polarizations, but not for  $(a', b')$ . No new Raman-active phonon mode is expected by the structural phase transition from a cubic spinel to the tetragonal ( $C_{4h}$ ) phase. Energetically, the peak around 22 meV ( $180\text{cm}^{-1}$ ) can be assigned to the single magnon excitation observed in the in-

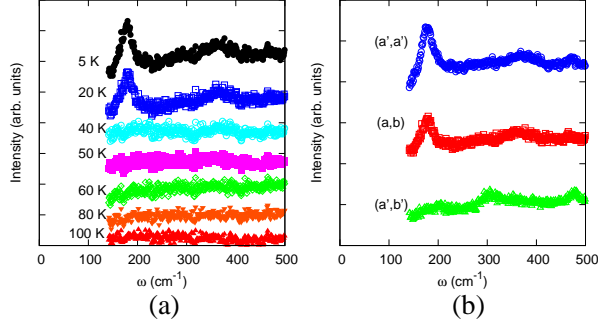


FIG. 1: (Color online) (a) Temperature dependence of Raman spectra for (a, b) light polarization. (b) Raman spectra for light polarizations (a', a'), (a, b), and (a', b') at 5K.

elastic neutron scattering experiment at  $\mathbf{q} = (2, 0, 2)$  [11]. The observed peak is a  $B_{2g}$  symmetry mode in the space ground  $D_{4h}$ . In this way, the peak is likely realized through the magnetic excitation processes.

However, the observed feature is unconventional as a magnetic scattering as shown below. As the possible conventional processes, we discuss (i) one-magnon excitation and (ii) simultaneous two-magnon excitation, which fail to explain the experimentally observed features. One-magnon scattering has been expected though the Raman tensor operator proportional to single spin term  $S_i^\alpha$  [14]. For the system where the inversion exist at the spin site, such a process can be active only for a cross light polarization. Thus, this synario is not consistent with the observation that the peak has been observed even in (a', a') light configuration (see Fig. 1 (b)). On the other hand, it is well known that the Raman tensor operator proportional to two spin term  $\mathbf{S}_i \cdot \mathbf{S}_j$  can induce the scattering due to simultaneous two-magnon excitations in Néel ordered state [14]. In this case, the spectra of two-magnon scattering reflect the density of states of two-magnon processes and, thus, the spectrum consists of asymmetric broad peak. In addition, the spectrum shape should depend on the light polarization. The observed peak in  $\text{MnV}_2\text{O}_4$  is likely a symmetric single peak, whose shape is almost identical for (a, b) and (a', a') configurations, and thus is unlikely two-magnon spectrum.

To explain the origin of the observed peak, we introduce a new mechanism to induce a Raman scattering process due to one-magnon excitation in noncollinear structures of spins. Let us consider the Raman process induced by a Heisenberg spin form tensor:

$$\hat{R} = \sum_{ij} \rho_{ij} (\mathbf{E}_I^\omega \cdot \mathbf{r}_{ij}) (\mathbf{E}_S^\omega \cdot \mathbf{r}_{ij}) (\mathbf{S}_i \cdot \mathbf{S}_j), \quad (1)$$

where  $\mathbf{r}_{ij}$  is the unit vector connecting spin  $i$  and  $j$ , and  $\mathbf{E}_I^\omega$  and  $\mathbf{E}_S^\omega$  are the incident and scattering light, respectively. The tensor (1) can be driven by the perturbation calculation in the Hubbard model [15, 16] and is domi-

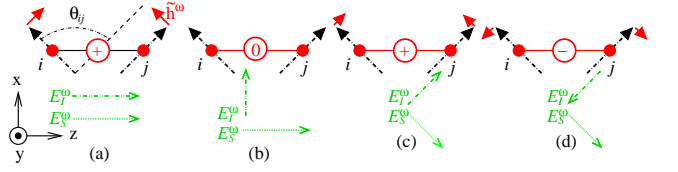


FIG. 2: (Color online) Effective fields  $\tilde{h}^\omega$  and spin directions are shown by small solid (red) and dash-dotted (black) arrows, respectively. The sign of  $(\mathbf{E}_I^\omega \cdot \mathbf{r}_{ij})(\mathbf{E}_S^\omega \cdot \mathbf{r}_{ij})$  on the bonds, which determine the direction of effective fields, are indicated. Light polarizations are (a)  $(E_I^\omega, E_S^\omega) = (x, x)$ , (b)  $(y, x)$ , (c)  $(x', -y')$ , and (d)  $(-x', -y')$ .

nant as a two spin term [13, 14, 17–19]. The coefficient  $\rho_{ij}$  depends on the exchange coupling  $J_{ij}$ . In the perturbation,  $\rho_{ij}$  is proportional to  $J_{ij}$  [15, 16]. In a collinear magnetic structure such as Néel ordered states, and also in a singlet gapped ground state, such a process can excite two magnon and bound state of triplets excitations rather than single magnon and triplet excitations, *i.e.* excitation satisfies the condition  $\Delta S \equiv S_e - S_0 = 0$  where  $S_0$  ( $S_e$ ) is a spin number of the ground (excited) state. However, in the noncollinear state, situation is dramatically changed so that one-magnon excitation by this process can contribute to the Raman scattering process.

To discuss the one-magnon scattering, let us rewrite the operator on the bond as  $\hat{R}_{ij} = (\tilde{\mathbf{h}}_i^{\omega(j)} \cdot \mathbf{S}_i + \tilde{\mathbf{h}}_j^{\omega(i)} \cdot \mathbf{S}_j)/2$  where  $\tilde{\mathbf{h}}_i^{\omega(j)} = \rho_{ij} (\mathbf{E}_I^\omega \cdot \mathbf{r}_{ij}) (\mathbf{E}_S^\omega \cdot \mathbf{r}_{ij}) \mathbf{S}_j$  is a local effective field coupled to  $\mathbf{S}_i$  and  $\tilde{\mathbf{h}}_j^{\omega(i)}$  vice versa. The effective field can be approximated as

$$\tilde{\mathbf{h}}_i^{\omega(j)} \sim \rho_{ij} (\mathbf{E}_I^\omega \cdot \mathbf{r}_{ij}) (\mathbf{E}_S^\omega \cdot \mathbf{r}_{ij}) \langle \mathbf{S}_j \rangle, \quad (2)$$

where  $\langle \mathbf{S}_j \rangle$  is an expectation value of the spin moment at site  $j$  on the ground state. When such an effective field has a transverse component with respect to the ground state spin direction, it is possible to make  $\Delta S = \pm 1$  excitation process, which induces the one-magnon excitation. The magnitude of the transverse component is represented by  $\tilde{h}_{i\perp}^{\omega(j)} = \rho_{ij} (\mathbf{E}_I^\omega \cdot \mathbf{r}_{ij}) (\mathbf{E}_S^\omega \cdot \mathbf{r}_{ij}) S \sin \theta_{ij}$  as a function of the relative angle  $\theta_{ij}$  between  $\mathbf{S}_i$  and  $\mathbf{S}_j$ . Since the transverse component proportional to  $\sin \theta_{ij}$ ,  $\tilde{h}_{i\perp}^{\omega(j)}$  vanishes for the collinear structure and becomes finite only for the noncollinear structure. Namely,  $\Delta S = \pm 1$  excitation can be induced when  $\mathbf{S}_i$  and  $\mathbf{S}_j$  are noncollinear. The effective field strongly depends on the light polarization through the term  $(\mathbf{E}_I^\omega \cdot \mathbf{r}_{ij})(\mathbf{E}_S^\omega \cdot \mathbf{r}_{ij})$ . As a result, in the case that both  $E_I^\omega$  and  $E_S^\omega$  have a components along the bond direction, the effective field can exist (see Fig. 2). Note that the direction of the effective fields can be reversed by changing the direction of  $\mathbf{E}_I^\omega$  or  $\mathbf{E}_S^\omega$  as shown in Figs. 2 (c) and (d).

As a whole, the local effective field at site  $\tilde{\mathbf{h}}_i^{\omega \text{ tot}}$  can be

written as

$$\tilde{\mathbf{h}}_i^{\omega tot} \equiv \sum_j \tilde{\mathbf{h}}_i^{\omega(j)} = \sum_j \rho_{ij}(\mathbf{E}_I^\omega \cdot \mathbf{r}_{ij})(\mathbf{E}_s^\omega \cdot \mathbf{r}_{ij})\langle \mathbf{S}_j \rangle, \quad (3)$$

where the summation of  $j$  is taken over all bonds connected to  $i$  site. When  $\tilde{\mathbf{h}}_i^{\omega tot}$  has a transverse component, the Raman process (1) couples to one-magnon excitation in ordered magnet. Once we know the ground state spin configuration, an activity of one-magnon Raman process and an induced magnon mode can be checked easily from Eq.(3). The selection rule can be understood from the light polarization dependence of the effective fields (3) as well. The Raman shift energy corresponds to the one-magnon excitation energy which can be evaluated by applying a conventional linear spin wave theory. Here excited magnon wavenumber  $\mathbf{q}$  can be obtained from the Fourier transforms of the effective field  $\tilde{\mathbf{h}}_i^{\omega tot}$ . Note that, when we consider the magnon dispersion in a reduced Brillouin zone of the magnetically ordered state, such a wave number  $\mathbf{q}$  must exist at  $\Gamma$  points.

Let us now bring the argument back to the topics on  $\text{MnV}_2\text{O}_4$ . As shown in Fig. 3 (a), a noncollinear ground state structure has been observed in the neutron scattering experiment [9]. In this compound, the strongest super exchange interaction exists on the bond along [110] and  $[\bar{1}\bar{1}0]$  directions between V sites ( $J_{BB}$  bond in Fig. 3 (a)). Thus, we consider the Raman process on this bond. From the figure, we can easily obtain that one-magnon Raman process is active in this compound, and two types of magnon process can be induced for  $(x, x)$  and  $(x, y)$  light polarizations. Each mode can be assigned to  $A_{1g}$  and  $B_{2g}$  symmetry mode respectively in the space group  $D_{4h}$ . Effective fields of each magnon mode are shown in Figs. 3 (b) and (c). Since  $(x', x')$  polarization contains  $A_{1g} + B_{2g}$  symmetry, both magnon modes produce the Raman scattering. On the other hand,  $(x', y')$  polarization does not couple to the one-magnon scattering since one of the components is orthogonal to the bond direction as in Fig. 2 (b). From the symmetry of light polarization, the experimentally observed  $B_{2g}$  mode at  $180\text{cm}^{-1}$  can be assigned to the one-magnon mode in Fig. 3 (c) and the peak structure in Raman spectra for  $(a, b)$  light polarization is likely realized due to  $(x, y)$  configuration rather than  $(z, x)$ . The selection rule for the present mechanism predicts that the other mode in Fig. 3 (b) exists at lower energy.

To confirm the peak position of each magnon mode, we consider the magnetic features in the spin Hamiltonian for  $\text{MnV}_2\text{O}_4$  [11]:

$$\mathcal{H} = \sum_{n.n.} \tilde{J}_{ij} \tilde{\mathbf{S}}_i \cdot \tilde{\mathbf{S}}_j + \sum_{i\alpha} \tilde{D}_i^\alpha (\tilde{S}_i^\alpha)^2, \quad (4)$$

where  $\tilde{\mathbf{S}}_i$  is an  $S = 1$  spin operator and interactions are defined as  $\tilde{J}_{ij} = J_{ij} S_i S_j$  and  $\tilde{\mathbf{D}} = \mathbf{D}(S_i)^2$ . The nearest neighbor interactions between  $A$  and  $B$  are defined as  $\tilde{J}_{AB}$  and those between  $B$  ions  $\tilde{J}_{BB}$  and  $\tilde{J}'_{BB}$

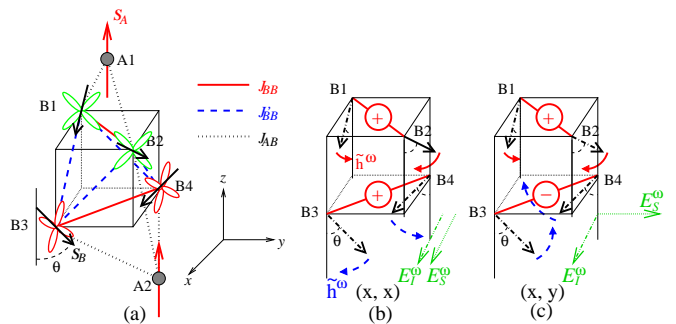


FIG. 3: (Color online) (a) Magnetic structures and exchange interactions  $J_{AB}$ ,  $J_{BB}$ , and  $J'_{BB}$  for  $\text{MnV}_2\text{O}_4$ . Ground state spin structures are shown. Orbital order structure on  $B$ -sites are also indicated:  $d_{yz}$  on  $B1$  and  $B2$  sites and  $d_{zx}$  on  $B3$  and  $B4$  sites. (b) Effective fields for  $V$  spins with light polarizations  $(x, x)$  and (c)  $(x, y)$ . The solid (dashed) arrows in  $zx$  ( $yz$ ) plane. The dash-dotted arrows indicates the spin direction on the ground states.

as shown in Fig. 3 (a). The single ion anisotropy term at each spin site is also introduced as  $\tilde{\mathbf{D}}_A$  and  $\tilde{\mathbf{D}}_B$ , respectively. We assume the spin structures estimated from the neutron scattering experiment [9]:  $\tilde{S}_{A1} = (0, 0, 1)$ ,  $\tilde{S}_{A2} = (0, 0, 1)$ ,  $\tilde{S}_{B1} = (\sin \theta, 0, -\cos \theta)$ ,  $\tilde{S}_{B2} = (-\sin \theta, 0, -\cos \theta)$ ,  $\tilde{S}_{B3} = (0, \sin \theta, -\cos \theta)$ , and  $\tilde{S}_{B4} = (0, -\sin \theta, -\cos \theta)$ . The angle  $\theta$  is given by  $\cos \theta = 6\tilde{J}_{AB}/(4\tilde{J}_{BB} + 4\tilde{J}'_{BB} + 2\tilde{D}_B^z - \tilde{D}_B^x - \tilde{D}_B^y)$  to minimize the classical ground state energy. The orbital ordering of  $d_{yz}$  and  $d_{zx}$  on  $B$ -sites, *i.e.*,  $V$ -sites, observed in Refs. 8 and 9 is also shown in the figure.

To reproduce the magnetic behaviors in  $\text{MnV}_2\text{O}_4$ , we adopt the interactions:  $\tilde{J}_{BB} = 14.0$  meV ( $113$   $\text{cm}^{-1}$ ),  $\tilde{J}_{AB}/\tilde{J}_{BB} = 0.18$ ,  $\tilde{J}'_{BB}/\tilde{J}_{BB} = -0.15$ ,  $\tilde{D}_A^z/\tilde{J}_{BB} = -0.01$  for  $A$  site ions,  $\tilde{D}_B^\beta = -0.15$  ( $\beta = x$  for  $B1$  and  $B2$  sites  $y$  for  $B3$  and  $B4$ ), and  $\tilde{D}_B^z = 0.2$  for  $B$  site ions. The other components of  $\tilde{\mathbf{D}}$  are taken to be zero. Calculated dynamical structure factor  $S(\mathbf{q}, \omega)$  along  $(4-l, 0, l)$  and  $(2, 0, l)$  by the linear spin wave theory is reasonably consistent with experimental data observed in neutron scattering experiments [11]. As a typical case, the structure factor  $S(\mathbf{q}, \omega)$  at  $\mathbf{q} = (2, 0, 2)$  in Ref. 11 corresponds to the two peaks structure in this energy range).  $\tilde{J}'_{BB}$  is taken as a ferromagnetic interaction, which is reasonable for the antiferro-orbital ordering state [12, 20]. In our model, the canted angle  $\theta$  for the  $V$  moment is about  $75^\circ$ , which is reasonably consistent with the value  $65^\circ$  estimated from neutron scattering experiments [9]. Note that the magnetic excitations obtained in the given parameters give the much better agreement with the experimental results than those in the parameters with  $\theta = 65^\circ$ .

Let us consider the magnetic excitation at  $\Gamma$  points (Magnon dispersion along  $(0, 0, l)$  is shown in Fig. 4 (a)).

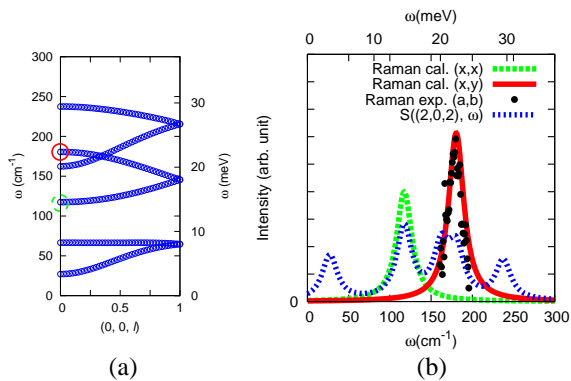


FIG. 4: (Color online) (a) Magnon dispersion for the present model along  $(0,0,1)$  direction. Raman active energy for  $(x,y)$  ( $(x,x)$ ) light polarization is indicated by red solid (green dashed) circles. (b) Raman shifts intensities for  $(x,x)$  and  $(x,y)$  light polarizations, and  $S(\mathbf{q},\omega)$  at  $\mathbf{q} = (2,0,2)$ . The delta function is replaced by the Lorentzian with width  $\epsilon/\bar{J}_{BB} = 0.1$ . The peak observed experimentally for  $(a,b)$  light polarizations at 5K (experimental results between  $160 \text{ cm}^{-1}$  and  $195 \text{ cm}^{-1}$ ) is also shown.

Lowest two energy modes ( $30$  and  $80 \text{ cm}^{-1}$ ) are due to oscillations of  $S_A$  spins and the other four modes are mainly caused by vibrations of  $S_B$  spins as observed in related spinel  $\text{Mn}_3\text{O}_4$  [11]. The magnon excitation around  $180 \text{ cm}^{-1}$  has the magnon mode in Fig. 3 (c), which is in agreement with our assignment from the symmetry of light polarizations. The magnon mode for  $(x,x)$  (the mode in Fig. 3 (b)) is expected to exist at lower frequency around  $120 \text{ cm}^{-1}$ . Experimental observation at lower frequencies will be the test of the validity of our theory.  $(x',x')$  light polarization consist of both  $(x,x)$  and  $(x,y)$  features. Thus, for this configuration, two peaks are expected, and the higher energy peak is consistent with the experimental observation. Theoretically, there is no peak due to one magnon process for  $(x',y')$  configuration as the experimental observation in the energy range  $\omega \gtrsim 150 \text{ cm}^{-1}$ . The peaks in Raman spectra due to one-magnon process calculated for  $(x,x)$  and  $(x,y)$  light polarizations, and the experimentally observed peak for  $(a,b)$ , which is likely produced by  $(x,y)$  light polarization, are shown in Fig. 4 (b). In our theory, there is no magnetic scattering due to one magnon process for light polarizations on the  $yz$  and  $zx$  plane except for  $(x,x)$  and  $(y,y)$ . Thus, experiments on the surfaces fixed in the tetragonal setting also give the crucial test to our theory.

To summarize, we propose a new mechanism to induce one-magnon Raman scattering process in noncollinear magnets. Such a one-magnon process for a certain light polarization can detect a single one-magnon mode at  $\Gamma$  point, where several modes are folded within the reduced zone. One of the advantages of the Raman scattering is

that it is sensitive to the symmetry of the magnon mode so that, together with the selection rules, it clarifies microscopic details of the magnon excitations. On the other hand, neutron scattering experiments detect the magnon dispersions throughout the Brillouine zone with less sensitivity to the symmetry. Thus, both methods play complementary roles to investigate the magnetic excitations in noncollinear magnets. In the present case, we indeed obtain the spin exchange couplings which matches the orbital-order patterns of  $\text{MnV}_2\text{O}_4$ .

One-magnon Raman scattering process observed in  $\text{MnV}_2\text{O}_4$  can also exist in a wide range of magnetic materials, especially in frustrated magnets with noncollinear spin structures. For example, such Raman processes are likely observable in two-in two-out structures realized in the spin ice materials [1, 21, 22] and parasite ferromagnetic states as observed in  $\alpha\text{Fe}_2\text{O}_3$  above Morin temperature [23]. The possibility in the other materials can be discussed by the same procedure in  $\text{MnV}_2\text{O}_4$ .

In this Letter, we restrict the tensor operator in Eq. (1). Even in the case of reduced symmetries, *e.g.* the effects of the polarization perpendicular to the bond can not be neglected, we can treat the process using a general form for Raman operator in Ref. 14 in a similar fashion.

We thank R. Kubota, N. Kida, T. Arima, R. Shimano, Y. Segawa, and Y. Tokura for fruitful discussion. This work is in part supported by Grant-In-Aids for Scientific Research from the Ministry of Education, Culture, Sports, Science and Technology (MEXT) Japan.

- 
- [1] A. Ramirez et al., Nature **399**, 333 (1999).
  - [2] T. Kimura et al., Nature (London) **426**, 55 (2003).
  - [3] S.-H. Lee et al., Nature Materials **6**, 853 (2007).
  - [4] C. Castelnovo, R. Moessner, and S. L. Sondhi, Nature **451**, 1184 (2008).
  - [5] P. W. Anderson, Phys. Rev. **102**, 1008 (1956).
  - [6] R. Plumier and M. Sougi, Solid State Communications **64**, 53 (1987).
  - [7] R. Plumier and M. Sougi, Physica B **155**, 315 (1989).
  - [8] T. Suzuki et al., Phys. Rev. Lett. **98**, 127203 (2007).
  - [9] V. Garlea et al., Phys. Rev. Lett. **100**, 066404 (2008).
  - [10] Adachi et al., Phys. Rev. Lett. **95**, 197202 (2005).
  - [11] J.-H. Chung et al., Phys. Rev. B **77**, 054412 (2008).
  - [12] H. Tsunetsugu and Y. Motome, Phys. Rev. B **68**, 060405 (2003).
  - [13] R. Elliott and R. Loudon, Physics Letters **3**, 189 (1963).
  - [14] T. Moriya, J. Phys. Soc. Jpn. **23**, 490 (1967).
  - [15] B. S. Shastry and B. I. Shraiman, Phys. Rev. Lett. **65**, 1068 (1990).
  - [16] F. Vernay, T. Devereaux, and M. Gingras, J. Phys.: Condens. Matter **19**, 145243 (2007).
  - [17] P. Lemmens et al., Phys. Rev. B **55**, 15076 (1997).
  - [18] P. Lemmens et al., Phys. Rev. Lett. **85**, 2605 (2000).
  - [19] P. Lemmens, G. Güntherodt, and C. Gros, Physics Reports **375**, 1 (2003).

- [20] In Ref. [11], the interaction  $\tilde{J}'_{BB}$  has been estimated to be antiferromagnetic under the assumption of the ferro-orbital ordering. Note that the work has been done prior to the experimental determination of magnetic and orbital structures [9].
- [21] M. Hariis et al., Phys. Rev. Lett. **79**, 2554 (1997).
- [22] S. Bramwell et al., Phys. Rev. Lett. **87**, 047205 (2001).
- [23] F. Morin, Phys. Rev. **78**, 819 (1950).